Ferromagnetic resonance study of GdN thin films with bulk and extended lattice constants

K. Khazen, H. J. von Bardeleben,* and J. L. Cantin
Institut des Nanosciences de Paris (INSP), Universités Paris 6&7, UMR 7588 au CNRS 140, rue de Lourmel, 75015 Paris, France

A. Bittar,[1] S. Granville,[2] H. J. Trodahl,[2] and B. J. Ruck[2]
[1]*MacDiarmid Institute of Advanced Materials and Nanotechnology, Industrial Research Ltd., PO Box 1313, Lower Hutt, New Zealand*
[2]*MacDiarmid Institute of Advanced Materials and Nanotechnology, Victoria University of Wellington, PO Box 600, Wellington, New Zealand*

(Received 22 May 2006; revised manuscript received 14 September 2006; published 27 December 2006)

The magnetic properties of GdN thin films with bulk and 2.4% extended lattice parameters have been studied by x-band ferromagnetic resonance (FMR) spectroscopy. Simple, anisotropic, single line FMR spectra are observed in the 0 to 18 kOe field range. Both films show an in-plane easy axis of magnetization due to the predominance of the shape related demagnetization fields. The films deposited on (100) Si substrates are strained with uniaxial anisotropy constants up to $K_u = +5 \times 10^6$ erg/cm^3 at $T = 4$ K. The lattice extension reduces the magnetization and decreases the Curie temperature from 69 K for the bulk films to 20 K for the films with extended lattice constants. Highly increased FMR linewidths are observed for the lattice extended films indicating large, local variations of the demagnetization fields.

DOI: 10.1103/PhysRevB.74.245330 PACS number(s): 76.50.+g, 75.50.Pp, 75.50.Dd

INTRODUCTION

3*d* transition metal (TM) doped 3-5 and 2-6 based ferromagnetic (FM) semiconductors are actively studied due to their potential application in spintronics. The realization of these materials raises a number of problems due to the limited solubility of the TM ions in the zincblende or wurtzite structures and the requirement of high carrier concentrations necessary for the establishment of the FM phase. The rare earth pictnide GdN is an interesting alternative as it does not require doping with magnetic ions, naturally introduced by the Gd ions, nor does it apparently require extrinsic doping and a high carrier concentration to achieve the ferromagnetic phase. After some early studies in the 60's and 70's, GdN has recently become the object of a series of theoretical and experimental studies.[1–12]

GdN crystallizes in the rocksalt structure with all Gd ions being in the 3^+ charge state, i.e., a $4f^7$ electron configuration with a ground state $^8S_{7/2}$. The lattice constant of stoichiometric GdN is 4.998 Å but oxygen contamination has been reported to decrease this value. A further consequence of oxygen contamination is an increase in the magnetic fields required to saturate the magnetization: whereas intrinsic GdN saturates at fields of ~5 kOe, this value is increased to several 10^4 Oe for a few percent oxygen contamination. Due to an easy oxygen uptake when exposed to air, it is difficult to produce high quality stoichiometric single crystals and the material has been studied very little experimentally.

The band structure of GdN has been calculated by different authors.[3–6] It is reported to be a small gap semiconductor in the paramagnetic phase. In the FM phase the minimum gaps were found to be indirect with a gap of 0.3 eV for the majority spins and 1.4 eV for the minority spins.[6] The corresponding minimum direct gaps at Γ are 0.8 and 1.6 eV, respectively.[6] The band structure of this material is predicted to be magnetic field and magnetic phase dependent.[4] In addition, the electronic structure of GdN has been predicted to be influenced by strain[2] but experimental results are not yet available. Its Curie temperature is 68 K.

Concerning the electronic properties, no clear picture has emerged. Widely varying room temperature carrier concentrations between 10^{18} and 10^{21} cm^{-3} have been reported[1,10] and both nitrogen vacancies and oxygen donors have been proposed as a source for free carriers. But no conclusive identification relating the carrier concentration to any of these defects has been achieved. Conflicting results have also been reported concerning its half-metallic or semiconducting nature in the ferromagnetic state ($T < 68$ K). Above the Curie temperature, it is an indirect small gap semiconductor displaying a thermally activated conductivity: activation energies varying between 1 and 10 meV have been reported.[1,7] It is an open question whether the activation energy corresponds to a particular defect level or whether it is the activation energy for hopping conductivity in a degenerate impurity band. Contrary to the similar FM compound EuO, its resistivity changes only by a factor of ~2 at the Curie temperature.[1] Irrespective of the different carrier concentrations, the magnetization measurements on GdN bulk single crystals have shown very similar results with a saturation magnetic moment of ~7 μ_B/Gd atom and Curie temperatures of 60–70 K.[1,8–12]

Contrary to GdN bulk material the magnetic properties of thin films have been much less studied.[1,7] Their properties may differ from those of bulk crystals due to strain and surface and grain size effects for nanocrystalline films. In particular, in the case of heterostructures, such as our case of GdN on (100)Si, the microstructure of the layer will have important consequences for its magnetic properties. Lattice mismatch related strain is expected to change the lattice constants and to introduce uniaxial anisotropies. A recent study of Duan *et al.*[2] has shown the importance of such effects also for the electrical properties with a strain induced half-metal to semiconductor transition and a change of the Curie temperature. It has also been shown recently that the lattice pa-

rameter of the GdN film is sensitive to the deposition temperature and that films with several percent increased lattice constants can be obtained.[13] As expected, this change in the lattice constants will modify the magnetic properties of the film and in particular decrease the Curie temperature. However, the origin of the increased lattice constants has not been clarified.

Ferromagnetic resonance spectroscopy (FMR)[14] is an interesting technique to probe the magnetic properties of thin GdN films as it has a sufficiently high sensitivity, in fact down to a few monolayers, and provides information on parameters such as the effective magnetization, the magnetic anisotropy constants, and the layer microstructure. We report here a FMR study of thin GdN films with bulk and extended lattice constants.

EXPERIMENTAL DETAILS

Two types of GdN thin films have been prepared under ultrahigh vacuum (UHV) conditions: type I films were obtained by thermal evaporation of Gd in a N_2 atmosphere and type II films by ion beam assisted deposition. For details of the sample preparation see Ref. 7. The deposition temperature was close to room temperature. The samples with a typical thickness of 200 nm were deposited on (100) oriented Si substrates. The films were polycrystalline with typical grain sizes of 10 nm (type I) and 3 nm (type II). The lattice constants of the thermally evaporated films $a=5.01$ Å are close to the bulk values ($a=4.998$ Å), whereas the ion beam assisted films show a 2.4% increased lattice constant of $a=5.12$ Å. To protect the films from oxygen contamination during the *ex situ* FMR measurements, they were capped in the UHV growth setup by a 200 nm nanocrystalline GaN film. The two types of GdN films showed very different electrical properties with resistivities at 300 K of 0.3 Ω cm and 70 Ω cm, respectively. The films with the bulk lattice constants show a thermally activated electrical conductivity in the paramagnetic phase with a minimum at the Curie temperature at 69 K. The films with the extended lattice constants present a monotonous decrease of the conductivity down to $T=10$ K with no particular change at the Curie temperature.

The FMR measurements were performed with a standard x-band spectrometer in the 4.5 to 300 K temperature range. 100 kHz field modulation and phase sensitive detection were employed, which gives first derivative absorption spectra characterized by their lineshape, peak-to-peak linewidth, and their resonance position. The dc magnetic field was varied between 0 and 18 kOe. The samples of typical dimensions of 3×3 mm are mounted in the center of a rectangular TE_{102} cavity. Typically, the FMR spectra were measured for rotations of the applied magnetic field in plane and out of plane.

The FMR spectra were analyzed in the Smit-Beljers formalism[15] for a thin film of cubic symmetry allowing for a possible uniaxial deformation related to the lattice mismatch between the GdN and the underlying (100) Si substrate. The energy density for this case is[16]

$$E = -MH + K_1(\alpha_1^2\alpha_2^2 + \alpha_2^2\alpha_3^2 + \alpha_3^2\alpha_1^2) + (2\pi M^2 - K_u)\alpha_2^2, \tag{1}$$

which represent the Zeeman interaction, the magnetocrystalline anisotropy energy, and the demagnetization energy; K_1 is the fourth order cubic magnetocrystalline anisotropy constant, K_u the second order uniaxial anisotropy constant, α_i the direction cosines of the magnetization M relative to the cubic crystal axes, and H the applied field. Taking the film plane as the x-z plane (Fig. 1) we obtain the following resonance conditions from the Smit-Beljers equations:

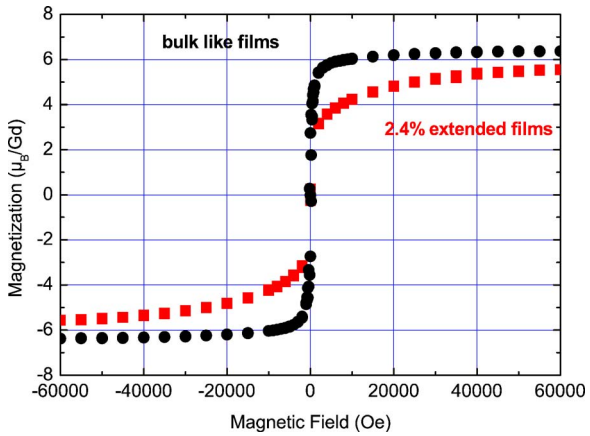

FIG. 1. (Color online) Static magnetization curves at $T=4$ K for bulk type I (black circles) and 2.4% lattice extended type II GdN (red squares) films.

$$\frac{\partial E}{\partial \varphi} = 0 \quad \frac{\partial E}{\partial \theta} = 0 \tag{2}$$

$$\left(\frac{\omega}{\gamma}\right)^2 = \frac{1}{M^2 \sin^2\theta}\left\{\frac{\partial^2 E}{\partial \theta^2}\frac{\partial^2 E}{\partial \varphi^2} - \left[\frac{\partial^2 E}{\partial \varphi \partial \theta}\right]^2\right\}. \tag{3}$$

For the out-of-plane measurements ($\theta=\pi/2$), the static equilibrium orientation of the magnetization is given by

$$H\sin(\varphi_H - \varphi) = 4\pi M_{eff}\sin(\varphi)\cos(\varphi) + \frac{K_1}{2M}\sin(4\varphi), \tag{4}$$

and the resonance field by

$$\left[\frac{\omega}{\gamma}\right]^2 = \left[H\cos(\varphi_H - \varphi) - 4\pi M_{eff}\sin^2\varphi + \left(\frac{K_1}{M}\right)(2 - \sin^2 2\varphi)\right],$$

$$\left[H\cos(\varphi_H - \varphi) + 4\pi M_{eff}\cos(2\varphi) + \frac{2K_1}{M}\cos 4\varphi\right]. \tag{5}$$

For the in-plane FMR measurements, the equivalent equations are

$$H\sin(\varphi_H - \varphi) = \frac{K_1}{2M}\sin(4\varphi) \tag{6}$$

and

$$\left[\frac{\omega}{\gamma}\right]^2 = \left[H\cos(\varphi_H - \varphi) + 4\pi M_{eff} + \left(\frac{K_1}{M}\right)(2 - \sin^2 2\varphi)\right],$$

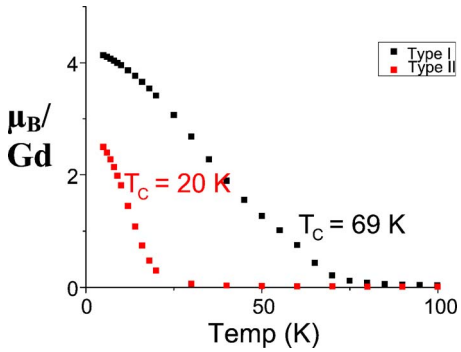

FIG. 2. (Color online) Temperature dependence of the magnetization at $H=500$ Oe for type I and type II GdN films.

$$\left[H\cos(\varphi_H-\varphi)+\frac{2K_1}{M}\cos 4\varphi\right], \tag{7}$$

$$\text{with}\quad 4\pi M_{eff}=4\pi M-2\frac{K_u}{M}\quad\text{and}\quad M=M(H,T). \tag{8}$$

EXPERIMENTAL RESULTS

Magnetization measurements

The static magnetization of the two films was measured with a superconducting quantum interference device (SQUID) for an in-plane orientation of the magnetic field. Our results show (Figs. 1 and 2) a difference both in the magnetization and the Curie temperature of the two films: the bulk type I films have a maximum magnetization M_{sat} of 6.4 μ_B/Gd which is only slightly lower than the highest values reported for bulk crystals. The magnetization saturates for applied fields of ~5 kOe. The type II films with the extended lattice constant show a strongly reduced magnetization of 4.3 μ_B/Gd at 10 kOe, as compared to 6.4 μ_B/Gd at 10 kOe for the type I films. The saturation of the magnetization requires applied fields of more than 40 kOe indicating a high degree of disorder. The Curie temperature is also drastically reduced for the type II films from 69 to only 20 K.

Ferromagnetic resonance results

The geometry of the FMR measurements is shown in Fig. 3. The thin film lies in the x-z plane, and angular variation of the FMR spectra are measured for in-plane (x-z) and out-of-plane (x-y) rotations of the applied magnetic field. For a general, oblique orientation of the magnetic field relative to the film plane, the applied field and the magnetization are no longer collinear.

TYPE I FILMS WITH BULKLIKE LATTICE CONSTANTS

In Fig. 4 we show a typical FMR spectrum measured at $T=15$ K with the orientation of the magnetic field H normal to the film plane. At all temperatures below T_c, the FMR spectrum is composed of a single line of typically 1 kOe peak-to-peak width. The spectrum is axially symmetric and

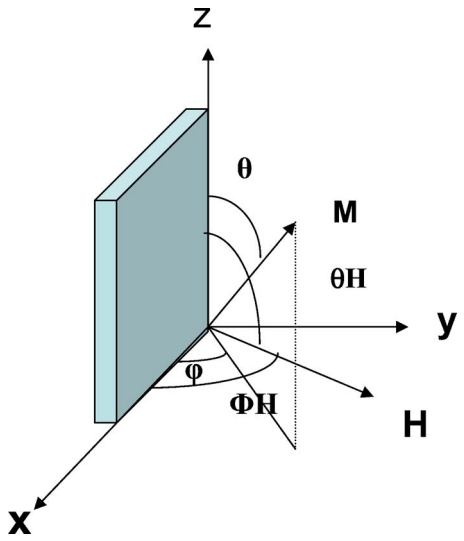

FIG. 3. (Color online) Magnetic field H and magnetization M orientation in the xyz coordinate system; film plane is (xz), the out-of plane variation of the magnetic field is in the (xy) plane.

extends at $T=4$ K from 0.6 kOe (H in plane) to 18 kOe ($H\perp$ plane). The large deviation from the paramagnetic $g=2$ value of 3340 Oe is due to the strong demagnetization fields related to the thin film geometry and the magnetocrystalline anisotropy. The observation of a single line spectrum proves the homogeneity of the magnetic properties of these films. The slightly asymmetric lineshape, related to the high conductivity of the film, can be well simulated by a mixed absorption/dispersion shape (Fig. 4). The symmetric shape and the small width of 850 Oe of the resonance line at $T=15$ K is remarkable for a nanocrystalline film and must be ascribed to a uniform stress in the film and possibly also a textured nature of the layer. The in-plane resonances occur (Fig. 5) at low magnetic fields of ~600 Oe. For the determination of the in-plane resonance fields for which $H_{res}\approx\Delta H_{pp}$, both resonance and antiresonance terms have been considered in order to determine the value of the resonance field.[17]

The out-of-plane angular variation of the resonance fields at $T=4$ K (Fig. 5) can be well simulated with Eqs. (4) and

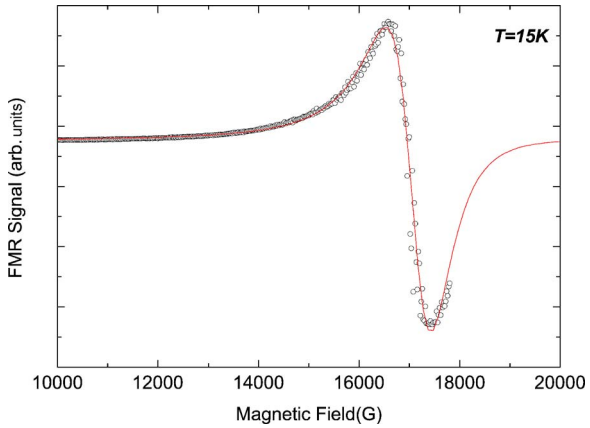

FIG. 4. (Color online) FMR spectrum of type I GdN for H out-of-plane and $T=15$ K; experimental points (○), simulated lineshape (line).

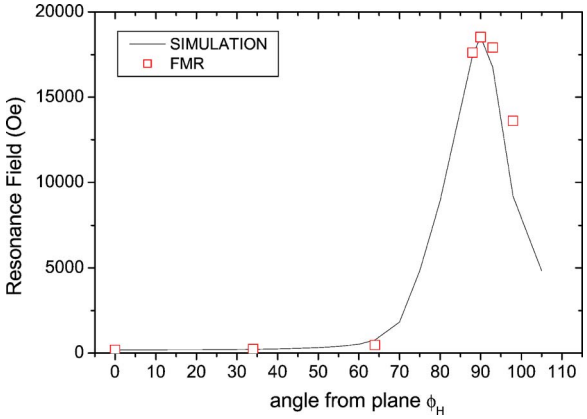

FIG. 5. (Color online) Angular variation of the resonance fields of type I GdN as a function of the angle between the applied field and the film plane at $T=4$ K; points: experimental, line: simulated angular variation with parameters: $M_{19000\ G}=1768$ emu/cm^3, $K_u=5.09\times10^6$ erg/cm^3, $K_1=1.14\times10^6$ erg/cm^3.

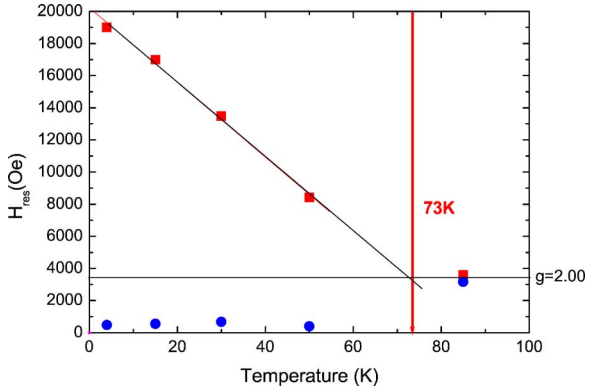

FIG. 6. (Color online) Temperature dependence f, the resonance fields of type I GdN for out-of-plane (red squares) and in-plane (blue circles) field orientation; equally shown is the expected resonance field in the paramagnetic state (line).

(5). The axial symmetry with a maximum resonance field for H perpendicular to the film plane is imposed by the dominant shape anisotropy of the thin film. The easy axis of magnetization lies in the film plane for all temperatures. For the simulation of the angular dependence of the FMR spectra, it is essential to take into account the field dependence of the magnetization $M=M(H)$ which cannot be assumed to be constant at a fixed temperature. We then obtain the uniaxial and cubic anisotropy constants K_u and K_1 and the associated anisotropy fields $2\ K_{1,u}/M$ (Table I) from a fit of the resonance positions with Eqs. (4) and (5).

With the numerical values of 6.4 μ_B/Gd at $H=2$ T and 4.2 μ_B/Gd at $H=0.06$ T obtained from the SQUID measurements, we determine the second and fourth order magnetocrystalline anisotropy constants to $K_u=+5.09\times10^6$ erg/cm^3, $K_1=+1.14\times10^6$ erg/cm^3. The corresponding uniaxial anisotropy field $2K_u/M$ is 5759 Oe, i.e., much smaller than the demagnetization field of 22 kOe. The K_u term is a priori not expected for a cubic crystal; it must be attributed to a strain induced anisotropy often observed in thin films deposited on a structurally different substrate.

With increasing temperature, the in-plane and out-of-plane resonance fields approach the paramagnetic limit of 3350 Oe corresponding to $g=2.00$ (Fig. 6). From the temperature variation of the high field FMR line we can estimate the Curie temperature of the bulk film, and we obtain a value of 73 K which is in good agreement with the value of 69 K obtained from the static magnetization measurements. The Curie temperatures deduced from FMR measurements are expected to be higher, as they were measured in the presence of a magnetic field of $\geqslant$4 kOe.

The FMR linewidth is very sensitive to the microstructure of the films: any magnetic inhomogeneity is expected to increase the linewidth from that measured in a single crystal. Unfortunately, we do not know of any reference value for GdN bulk crystals, but values of 10^2 to 10^3 Oe are often encountered in x-band FMR of ferromagnetic semiconductors. In general, we can distinguish three contributions to the linewidth: the intrinsic linewidth, the anisotropy field induced broadening in polycrystalline layers, and the additional porosity/void induced broadenings. In the type I films we observe (Fig. 7) for the out-of-plane linewidth an increase with increasing temperature with a maximum close to the Curie temperature. This behavior is typical for FM thin films[14] in which the linewidth is not dominated by a distribution of the local demagnetization fields. As will be shown in the next section, a different behavior is observed for the type II films with extended lattice constants.

TYPE II FILMS WITH 2.4% EXTENDED LATTICE CONSTANTS

In Fig. 8 we show the FMR spectrum for the type II film at $T=10$ K for the orientation of the magnetic field normal to the film plane, and compare it with the spectrum observed for the bulk film at a comparable reduced temperature T/T_c. As in the previous case, we still observe a single resonance line for the orientations in plane and out of plane but the linewidth of the out-of-plane spectrum is strongly increased

TABLE I. Magnetization M, uniaxial anisotropy constant K_u, cubic anisotropy constant K_1, and the associated anisotropy fields for type I and type II GdN films

M (emu/cm^3)	$4\pi M$ (Oe)	K_u (erg/cm^3)	K_1 (erg/cm^3)	$2K_u/M$ (Oe)	$2K_1/M$ (Oe)	T (K)	GdN
1768	22220	5.09×10^6	1.14×10^6	5759	1292	4	type I
1243	15620	1.8×10^6	1.4×10^6	2897	2252	4	type II
200	2513	-1.4×10^5	-1.7×10^4	−1439	−172	20	type II

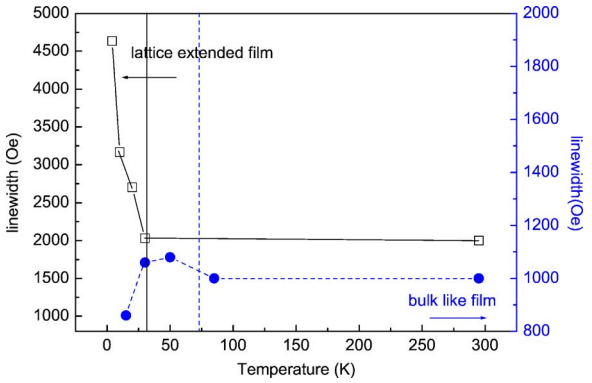

FIG. 7. (Color online) Out-of-plane linewidth as a function of temperature for type I films (right axis) and type II films (left axis); the FMR deduced Curie temperatures are indicated by vertical lines.

to 4700 Oe. The lineshape can equally be simulated by a mixed absorption/dispersion signal.

The FMR spectra show equally an axial symmetry of the resonance field with a maximum high field resonance for the out-of-plane orientation. Similar to the type I films, the easy axis of magnetization is lying in the film plane as the shape anisotropy is also dominating in these films. But the maximum and minimum resonance fields are reduced/increased as compared to the type I films mainly due to the lower magnetization of these films. For the simulation of the out-of-plane variation (Fig. 9), we have to take into account once again the even stronger field dependence of the magnetization $M(H)$. From a fit of the out-of-plane angular variation of the resonance positions, we obtain the anisotropy constants K_u, K_1: $K_u = +1.8 \times 10^6$ erg/cm^3, $K_1 = +1.4 \times 10^6$ erg/cm^3 (Table I). The same approach has been applied to the angular variation measured at $T=20$ K (Fig. 9) and the corresponding anisotropy constants are given in Table I. The film is still ferromagnetic at $T=20$ K under the applied magnetic field, but the magnetization (Fig. 2) and thus the resonance fields are strongly reduced.

The in-plane FMR spectra are isotropic. This is attributed to the polycrystalline character of the films, which if they were monocrystalline, should show the cubic in-plane anisotropy. The different lineshape and much larger width are indicative of disorder and structural defects in the lattice extended films; the ion bombardment during the film growth is expected to destroy any texturing of the film and might introduce macroscopic defects such as voids and increased grain boundary related disorder, all of which will give rise to strong variations of local magnetic properties. The FMR linewidth is known to be very sensitive to the homogeneity of the anisotropy fields which is modified by crystal defects such as stacking faults, twinning, and incomplete crystallization. Contrary to the case of the bulk films, we observe a reduction of the linewidth with increasing temperatures approaching a value of 2 kOe at 20 K (Fig. 10).

Nevertheless, the lowest value of 2000 Oe at $T \sim T_C$ is still significantly larger than that of type I films (Fig. 7). The larger width and its different temperature variation are an indication of porosity-related local demagnetization fields being the dominant contribution to the line broadening.

In Fig. 11, we plot the resonance field as a function of temperature; the extrapolation to the paramagnetic resonance field gives an approximate value of the Curie temperature of ~32 K.

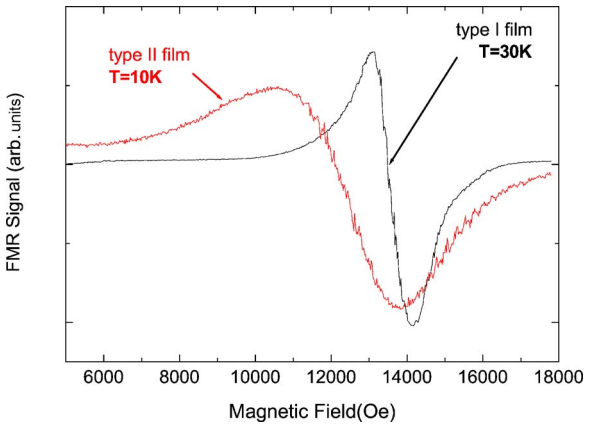

FIG. 8. (Color online) Comparison of out-of-plane FMR spectra for type I and II films.

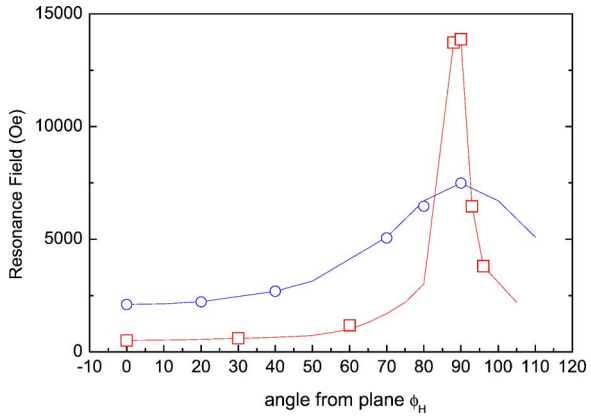

FIG. 9. (Color online) Angular variation of the resonance fields of type II films as a function of the angle between the applied field and the film plane at $T=4$ K (squares) and $T=20$ K (circles); the simulated variations are given as lines.

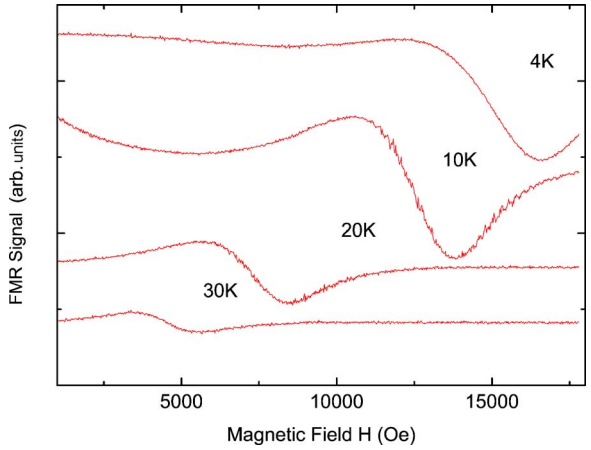

FIG. 10. (Color online) Out-of-plane FMR spectra of type II films as a function of temperature.

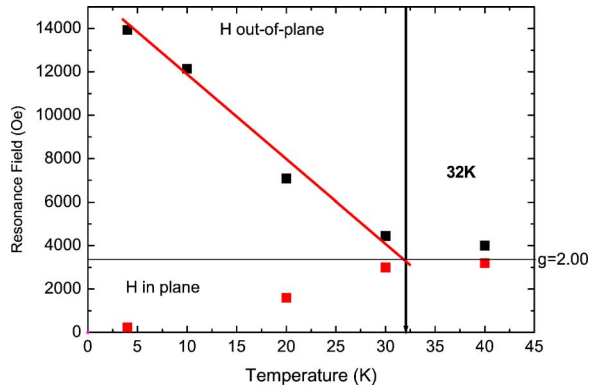

FIG. 11. (Color online) Temperature dependence of the resonance fields of type II films for out-of-plane and in-plane magnetic field orientation.

DISCUSSION

GdN thin films of bulk properties can be deposited on Si substrates by thermal evaporation under UHV conditions. Such films show well-resolved FMR spectra which allow an analysis of their magnetic properties. Ion assisted deposition leads to lower quality films with increased lattice constants. The FMR results show a dramatic effect of the lattice parameters and the structural quality of the films on the magnetic properties. We find for both types of films that the easy axis of magnetization is lying in the film plane due to the very strong demagnetization fields. The high value of the uniaxial magnetocrystalline constants is attributed to strain effects, which induce a tetragonal distortion of the lattice. This symmetry is a priori not expected for cubic materials, but is often observed in thin film deposited on substrates with a different crystal structure. The strain is higher for bulk films and then for the layers with extended lattice constants. The positive value of the parameter K_u indicates a compressive strain for both layers.

The average lattice parameters of our films are 0.4% (type I) and 2.4% (type II) higher than the ones reported for bulk crystals. This lattice extension should, according to Ref. 2 weaken the exchange interaction and thus lower the Curie temperature. According to these authors the increase in lattice constants from 5.01 to 5.12 Å reduces the first nearest neighbor ferromagnetic exchange energy from $J_1=-0.83$ meV to $J_1=-0.63$ meV, i.e. by 25%. In addition, the second nearest neighbor exchange energy J_2 becomes more antiferromagnetic and increases from +0.2 to +0.3 meV. The Curie temperature is proportional to the sum of the neighboring exchange energies $12\,J_1+6\,J_2$. Within this model, we would expect a reduction by a factor of 0.65 of the Curie temperature which gives $70\ \mathrm{K}\times 0.65=46$ K. This is in qualitative agreement with our observation, but our FMR spectra show that additional contributions related to the lower structural quality of the lattice extended films have equally to be taken into account.

The origin of the lattice parameter increase—equally reported in Refs. 13 and 18—has not yet been established, but it can be speculated that it is related to a high density of structural defects and disorder which is expected to be higher for the type II films grown under ion bombardment. To further investigate this problem, films grown with different ion bombardment energies will be grown. In addition, grain boundary effects are of increased importance in the type II films with nm grain size. In a recent publication,[13] the influence of the lattice expansion on the Gd $L_{2,3}$ absorption edges in GdN films with similar properties has been reported. In that study, films with a 4.4% increased lattice parameter and a grain size near 5 nm have been investigated. As in our case, no significant deviation from stoichiometry was observed in these layers. In fact, a high concentration of nitrogen vacancies is expected to make films highly conductive due to the donor nature of this defect which is not observed. These authors also report a reduction of the Curie temperature to $T_c=30$ K which is quite close to our value in spite of the higher increase of the lattice constants. They relate this change to an upward shift of the Gd 5*d* bands relative to the *N*-2*p* bands and a reduction of the exchange interaction. However, these authors have not considered the influence of structural defects in the films with extended constants.

TABLE II. Comparison of static magnetization at $T=4$ K and Curie temperatures for different thin film and bulk GdN materials

GdN	type I films bulk	type II films 2.4% extended	film/bulk
Ms at $T=4$ K and $H=60$ kOe $4\pi M_s$	6.4 μ_B/GdN (SQUID) 22 220 G	5.5 μ_B/Gd (SQUID) 15 620 G	6.8 μ_B/GdN[a] 7 μ_B/Gd 7.26 μ_B/Gd 26 000 G[b]
T_C	~73 K (FMR) 69 K (SQUID)	~32 K (FMR) 20 K (SQUID)	58 K[c] 69 K[d] 70 K[e] 30 K[f]

[a]Reference 1.
[b]Reference 11.
[c]References 1 and 8.
[d]Reference 19.
[e]Reference 12.
[f]Reference 13.

In Table II we compare the magnetic properties of our type I and type II films with those previously reported for thin films and bulk samples. We observe that the low temperature magnetizations of the thin films are always lower than the bulk values and decrease strongly for the films with extended lattice constants. The electrical conductivities of the samples seem to have much less influence on the magnetization and the Curie temperatures. A change from 0.01 (Ref. 1) to 0.3 Ω cm (our bulk films) in the room temperature resistivity modifies Ms by only 6%. This confirms previous conclusions that the carrier mediated RKKY interaction is only of minor importance for the ferromagnetic properties of GdN.

CONCLUSION

The FMR spectra of thin GdN films with bulk and extended lattice constants have been measured between 4 K

and the Curie temperatures. Both films show strong uniaxial strain with a second order anisotropy constant of $\sim 5 \times 10^6$ erg/cm^{-3} at 4 K. Due to the strong demagnetization fields, the easy axis of magnetization remains oriented in the film plane. The small linewidth and single FMR line observed for the bulk films show the good quality of these films with homogeneous magnetic properties. These films display magnetic properties comparable to those of bulk single crystals. The films obtained by ion beam assisted deposition have 2.4% extended lattice constants and a reduced Curie temperature of only 32 K. This result confirms the predictions by Duan *et al.*[2] of a reduced first nearest neighbor FM exchange interaction and a change of sign of the second nearest neighbor exchange interaction which becomes AF. The different FMR spectra of the type II films demonstrate that in addition to the lattice extension, the microstructure of the film has been degraded, giving rise to local variations of the demagnetization fields. The good signal to noise ratio of the FMR spectra of the bulk films would allow extending these measurements to ultrathin films of a few monolayer thickness for which surface effects and interface related strain effects could be explored.

ACKNOWLEDGMENTS

We acknowledge the support of a France–New Zealand cultural agreement contract. The work of the MacDiarmid Institute is supported by a New Zealand Centre of Research Excellence contract.

*Corresponding author. Electronic address: jurgen.vonBardeleben@insp.jussieu.fr

[1] F. Leuenberger, A. Parge, W. Felsch, K. Fauth, and M. Hessler, Phys. Rev. B **72**, 014427 (2005).
[2] C. Duan, R. F. Sabiryanov, J. Liu, W. N. Mei, P. A. Dowben, and J. R. Hardy, Phys. Rev. Lett. **94**, 237201 (2005).
[3] D. B. Gosh, M. De, and S. K. De, Phys. Rev. B **72**, 045140 (2005).
[4] M. Geshi, K. Kusakabe, and N. Suzuki, J. Phys.: Condens. Matter **16**, S5701 (2004).
[5] C. M. Aerts, P. Strange, M. Horne, W. M. Temmerman, Z. Szotek, and A. Svane, Phys. Rev. B **69**, 045115 (2004).
[6] W. R. L. Lambrecht, Phys. Rev. B **62**, 13538 (2000).
[7] S. Granville, B. J. Ruck, F. Budde, A. Koo, D. Pringle, F. Kuchler, A. Bittar, G. V. M. Williams, and H. J. Trodahl, Phys. Rev. B **73**, 235335 (2006).
[8] D. X. Li, Y. Haga, H. Shida, T. Suzuki, Y. S. Kwon, and G. Kido, J. Phys.: Condens. Matter **9**, 10777 (1997).
[9] D. X. Li, Y. Haga, H. Shida, and T. Suzuki, Physica B **199&200**, 631 (1994).
[10] P. Wachter and E. Kaldis, Solid State Commun. **34**, 241 (1980).
[11] R. A. Cutler and A. W. Lawson, J. Appl. Phys. **46**, 2739 (1975).
[12] R. J. Gambino, T. R. McGuire, H. A. Alperin, and S. J. Pickart, J. Appl. Phys. **41**, 933 (1970).
[13] F. Leuenberger, A. Parge, W. Felsch, F. Baudelet, C. Giorgetti, E. Dartyge, and F. Wilhelm, Phys. Rev. B **73**, 214430 (2006).
[14] M. Farle, Rep. Prog. Phys. **61**, 755 (1998).
[15] J. Smit and H. C. Beljers, Philips Res. Rep. **10**, 1113 (1955).
[16] R. Naik, C. Kota, J. S. Payson, and G. L. Dunifer, Phys. Rev. B **48**, 1008 (1993).
[17] K. Sugawara, C. Y. Huang, and B. R. Cooper, Phys. Rev. B **28**, 4955 (1983).
[18] F. Leuenberger, Ph.D. thesis, Universität Göttingen, 2004.
[19] D. P. Schumacher and W. E. Wallace, J. Appl. Phys. **36**, 984 (1965).